frontiers | Frontiers in Energy Research

ORIGINAL RESEARCH
published: 03 May 2022
doi: 10.3389/fenrg.2022.869404

The Stabilizing Effect of $Li_4Ti_5O_{12}$ Coating on $Li_{1.1}Ni_{0.35}Mn_{0.55}O_2$ Cathode for Liquid and Solid–State Lithium-Metal Batteries

Wei Hu, Shengwen Zhong, Xianfa Rao, Tingting Yan and Min Zeng*

Faculty of Materials Metallurgy and Chemistry, Jiangxi University of Science and Technology, Ganzhou, China

Li–rich layered cathode materials with high energy density suffer from severe capacity decay during cycling, which is associated with volume change and electrolyte corrosion during (de)lithiation. A Li^+ ionic conducting $Li_4Ti_5O_{12}$ coating with high structural integrity is developed on $Li_{1.1}Ni_{0.35}Mn_{0.55}O_2$ cathodes *via* a dry powder coating method. The electrochemical performances of $Li_4Ti_5O_{12}$–coated $Li_{1.1}Ni_{0.35}Mn_{0.55}O_2$ cathodes in liquid and solid–state lithium batteries were investigated. The initial discharge capacity of $Li_4Ti_5O_{12}$–coated $Li_{1.1}Ni_{0.35}Mn_{0.55}O_2$ in the liquid electrolyte has been improved from 116.5 mA h g^{-1} to 123.7 mA h g^{-1} at 0.1°C. An impressive cyclability with a high capacity retention of 89.3% was achieved in solid–state lithium batteries. These results demonstrate that the $Li_4Ti_5O_{12}$ coating plays an essential role in enhancing the specific capacity and better performance for $Li_{1.1}Ni_{0.35}Mn_{0.55}O_2$ cathode.

Keywords: cathode material, Li-ion battery, solid-state Li-metal battery, $Li_4Ti_5O_{12}$, coating

OPEN ACCESS

Edited by:
Henghui Xu,
Huazhong University of Science and Technology, China

Reviewed by:
Zhe Peng,
Ningbo Institute of Materials Technology and Engineering (CAS), China
Jun Zhang,
Zhejiang University of Technology, China
Nan Wu,
Beijing Institute of Technology, China

****Correspondence:***
Shengwen Zhong
Zhongshw@126.com

Specialty section:
This article was submitted to Electrochemical Energy Conversion and Storage, a section of the journal Frontiers in Energy Research

Received: *04 February 2022*
Accepted: *28 February 2022*
Published: *03 May 2022*

Citation:
Hu W, Zhong S, Rao X, Yan T and Zeng M (2022) The Stabilizing Effect of $Li_4Ti_5O_{12}$ Coating on $Li_{1.1}Ni_{0.35}Mn_{0.55}O_2$ Cathode for Liquid and Solid–State Lithium-Metal Batteries. Front. Energy Res. 10:869404. doi: 10.3389/fenrg.2022.869404

INTRODUCTION

Recently Li–rich cathode materials such as layered $LiNi_{1-x}M_xO_2$ ($0.1 < \times < 0.5$, M = Mn, Co., Al, etc.) have been widely investigated owing to their high specific capacity, excellent rate capability, low cost, and high output voltage (Hu et al., 2013; You and Manthiram, 2017; Nayak et al., 2018; Sun H. H et al., 2021). Generally, layered structured cathodes can be charged to 4.5 V and deliver an improved specific discharge capacity (Shi et al., 2018). However, the severe capacity decay and safety issues, especially at elevated temperature and high upper cutoff voltage, hindered their commercial application. Many mechanisms elucidating the deterioration of electrochemical performance during charge/discharge for layered structured cathodes have been proposed (Jung et al., 2014; de Biasi et al., 2019; Liu et al., 2020; Xu et al., 2020; Wang Y et al., 2020). The inherent defects, dissolution of Mn^{4+}/Ni^{4+} transition metals, gas release, phase transitions, volume change, electrolyte decomposition and corrosion, and formation of inactive interphases have imposed a negative impact on the electrochemical performance of the cathode materials. Notably, most decay mechanisms emphasize the unstable interface of the cathode and electrolyte. For instance, the voltage drop is associated with the formation of an insulating solid electrolyte interphase due to the oxidation decomposition of liquid electrolyte; the residual LiOH or Li_2CO_3 on the particle surface will lead to a deterioration of the specific discharge capacity, especially at high rates. Additionally, phase transition combined with volume contraction and expansion during (de) lithiation, the reduction of Ni^{4+} in a highly delithiated state, and oxygen loss may cause cracking and destroy the surface morphology of the cathode material (de Biasi et al., 2019; Sharifi-Asl et al., 2019; Sun J et al., 2021). Consequently, interior energy density and cycle life were obtained.

To solve these issues, surface modifications, including element doping and constructing a coating for the cathode material, have been widely employed to enhance the structure stability (Zhang et al., 2015; Kalluri et al., 2017; Xia et al., 2018; Nisar et al., 2020; Herzog et al., 2021a; Lin et al., 2021; Yan et al., 2021). Coatings such as Al_2O_3, TiO_2, Li_3PO_4, ZnO, $AlPO_4$, $LiAlO_2$, and Li_2ZrO_3 are an effective protective layer on the cathode particles for minimizing the surface side reactions and improving the cycle stability of Ni–rich layered cathodes. However, coatings with poor electric/ionic conductivities often impose an additional electrical and ionic transport resistance to cathode materials, which is detrimental to the Coulombic efficiency, specific charge–discharge capacity, and rate capability at high temperatures/upper cutoff voltages.

$Li_4Ti_5O_{12}$, having a high Li^+ ionic conductivity of 10^{-6} S cm^{-1} and superb structural stability, has been investigated as a desirable functional surface coating to facilitate Li^+ transport and enhance the electrochemical properties of electrode materials (Yan et al., 2021). $Li_4Ti_5O_{12}$ has the identical structure of spinel $LiMn_2O_4$, showing superior ability in the balance of surface protection and charge transfer during charge/discharge cycles (Yi et al., 2015; Zhou et al., 2016; Jia et al., 2018).

Effective strategies used to construct the surface coating layer on the cathode materials include subjecting the cathode materials to atomic layer deposition, radio–frequency (RF) magnetron sputtering, wet chemistry methods, chemical vapor deposition, followed by subsequent heating process (Liu et al., 2019). However, these methods are excessively subjected to expensive deposition instruments and low-yielding products, which show apparent disadvantages of high cost. Cost–effective and environmental–friendly dry powder coating approach is one of the widely studied methods and has been successfully used in industry to deposit Al_2O_3, TiO_2, $LiAlO_2$, and $Li_4Zr_3O_8$ coatings (Wang et al., 2018; Jiang et al., 2020; Herzog et al., 2021b). Ionic conductive $Li_4Ti_5O_{12}$ layer on the $LiCoO_2$ and $LiNi_xMn_yCo_zO_2$ surface showed excellently high–voltage stability, effectively suppressing structural degradation and facilitating lithium–ion diffusion for the $LiCoO_2$ cathodes (Wang C.-W et al., 2020; Herzog et al., 2021c). In this work, $Li_4Ti_5O_{12}$ coating on the $Li_{1.1}Ni_{0.35}Mn_{0.55}O_2$ particles was fabricated *via* a dry powder coating method, followed by a heating treatment during which nanosize TiO_2 *in situ* reacts with residual Li_2CO_3 on the surface of the as–prepared $Li_{1.1}Ni_{0.35}Mn_{0.55}O_2$ particles. Electrochemical performances are studied in both liquid and solid–state lithium batteries. It is found that the $Li_4Ti_5O_{12}$ coating enhances the rate capability and capacity retention of the $Li_{1.1}Ni_{0.35}Mn_{0.55}O_2$ electrodes in $LiPF_6$ electrolytes at various upper cutoff voltages and solid–state batteries at elevated temperatures.

MATERIALS AND METHODS

Materials Preparation and Characterization

The $Li_{1.1}Ni_{0.35}Mn_{0.55}O_2$ was prepared by a coprecipitation method with the brief description as follows: the stoichiometric amounts of nickel sulfate, manganese sulfate were first completely dissolved into deionized water, and the 3 mol L^{-1} sodium carbonate solution was added during mechanical stirring at room temperature. Subsequently, the mixture was transferred to a hydrothermal reactor and heated at 50°C for 20 h. After the cool down, the reaction was preserved at room temperature for 2 h. The final precursor was obtained by thoroughly washing the as–prepared precipitates. The obtained precursor was dried at 80°C under vacuum for 12 h, and then blended with a stoichiometric amount of lithium carbonate, pressed, and annealed at 500°C for 7 h in an alumina crucible in air. The black precursor was collected and ball–milled for a further 1 h; after sintering at 940°C for 12 h, the final product was quenched in air. The obtained $Li_{1.1}Ni_{0.35}Mn_{0.55}O_2$ was mixed with nanosize TiO_2, followed by heating at 800°C for 7 h to prepare $Li_4Ti_5O_{12}$ coated–$Li_{1.1}Ni_{0.35}Mn_{0.55}O_2$. The amount of titanium-containing coating was controlled with 1 wt%. The cooled powders were immediately sealed in a bottle under an argon atmosphere and stored in an argon–filled glovebox with H_2O < 0.1 ppm and O_2 < 0.1 ppm.

The microstructures of various powders were observed using scanning electron microscopy (FESEM, JEOLJSM–7600F) with 5 kV accelerating voltage, and X–ray diffraction data was collected on a Bruker D8 Advance X–ray diffractometer equipped with Cu–K_α radiation (1.54056 Å). The amounts of elements in powders were determined by inductively coupled plasma optical emission spectroscopy (ICP-OES) using a 720-ES (Varian, United States).

Electrode and Cell Preparation

The composite electrodes for conventional lithium battery were prepared by blending 90 wt% active material with 5 wt% poly (vinylidene difluoride) (PVDF) and 5 wt% Super P carbon black (CB) in N–methyl–2–pyrrolidone (NMP). To obtain uniform mixing of these ingredients, the mixture were loaded in a plastic bottle with four steel balls of 6.4 mm in diameter and kept rotating the bottle at 100 rpm for 12 h. The homogeneous slurry was cast on carbon–coated aluminum foil and dried in a vacuum oven at 60°C for 6 h and 120°C for 6 h to remove any residual NMP and moisture. Then it was punched into disks with a diameter of 12 mm and transferred into the Ar glovebox before use. The cathode loading was set to 7.0–8.0 mg cm^{-2} (120 mAh g^{-1} at a rate of 1 C). Lithium metal was used as the anode, and Celgard 2,500 was used as the separator. For the liquid electrolyte, 25 μl of a 1 M solution of $LiPF_6$ in ethylene carbonate (EC) and ethyl methyl carbonate (EMC) (50:50 w/w; SigmaAldrich) was used. In the case of all–solid–state cells, the composite electrodes were fabricated by using as–prepared active materials (70 wt%), poly (vinylidene fluoride) as the binder (10 wt %), LTFSI as the lithium salt (10 wt%), and acetylene black (10 wt%) as a conductive agent. PEO–based composite electrolytes (60 wt% LiTFSI in PEO (Mw = 600,,000 g mol^{-1})) were employed. All cells were assembled using CR2032 coin–type cells inside an argon-filled glove box with oxygen and water contents below 0.01 ppm.

Electrochemical Characterization

Electrochemical impedance spectroscopy (EIS) tests were performed for cells before and after cycling using a frequency response analyzer (Parstat 4,000, Princeton Applied Research)

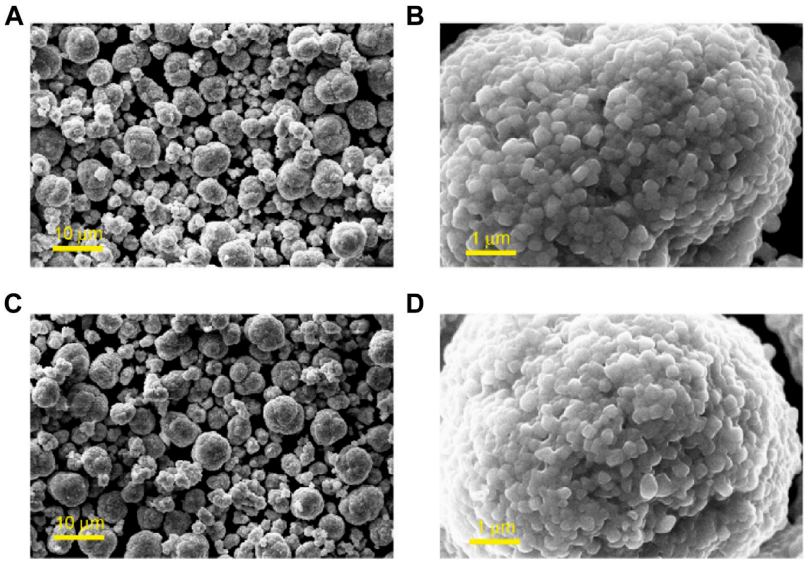

FIGURE 1 | SEM images of $Li_{1.1}Ni_{0.35}Mn_{0.55}O_2$ **(A,B)** pristine particles in different magnifications; and **(C,D)** particles with $Li_4Ti_5O_{12}$ coating in different magnifications.

with an amplitude of 10 mV. The frequency was set in the range from 10 kHz to 1 Hz. The cells after cycles were measured at the charged state of 4.3 V. Galvanostatic cell cycling was conducted at room temperature with a LAND battery testing system. The coin cells were rested for 48 h before cycling. Only the active material mass was considered for the calculation of the capacities and the specific currents. The C–rate was raised every four cycles during cycling, starting from 0.1/0.1 C (charge/discharge) to 0.3/0.3, 0.5/0.5, 1/1, 2/2, and 3/3 C. Afterward, for the long–term stability investigations, the cells were cycled at 0.5/0.5 C. The cycling performances of the all–solid–state cells were tested at 60°C.

RESULTS AND DISCUSSION

Figure 1 shows the SEM images of $Li_{1.1}Ni_{0.35}Mn_{0.55}O_2$ before and after the coating treatment, respectively. The obtained $Li_{1.1}Ni_{0.35}Mn_{0.55}O_2$ particles show spherical morphology with diameters ranging from 3 to 9 μm. The surface of the secondary particles is rough and consists of highly agglomerated primary crystals with sizes of ~300 nm. The morphology of $Li_{1.1}Ni_{0.35}Mn_{0.55}O_2$ particles maintains in good spherical shape after coating treatment, and no noticeable difference can be seen from the low–magnification, whereas, in the high–magnification SEM image (**Figures 1B,D**), the surface of the $Li_{1.1}Ni_{0.35}Mn_{0.55}O_2$ particles was smoother, and a thin of amorphous coating could be observed. ICP-OES results indicate that the Ti content in $Li_4Ti_5O_{12}$–coated $Li_{1.1}Ni_{0.35}Mn_{0.55}O_2$ cathode is approximately 1.2 wt%. The calculated weight percentage of Ni and Mn of as-prepared $Li_{1.1}Ni_{0.35}Mn_{0.55}O_2$ cathode is 21 and 31 wt%, respectively.

To investigate the influence of the coating materials on the cycling performance of $Li_{1.1}Ni_{0.35}Mn_{0.55}O_2$. The cells using liquid electrolytes were assembled to evaluate the rate capabilities first. As shown in **Figure 2**, rate measurement is performed at different rates; as the rate increases, the capacities of the samples decrease. The initial discharge capacities of pristine $Li_{1.1}Ni_{0.35}Mn_{0.55}O_2$ cathode at the incremental rates are 116.5, 115.9, 107.4, 97.7, 84.4 and 76.1 mAh g^{-1}. The $Li_4Ti_5O_{12}$–coated $Li_{1.1}Ni_{0.35}Mn_{0.55}O_2$ cathode delivers a capacity of 123.7, 124.8, 117.2, 109.9, 97.2 and 88.1 mAh g^{-1} at 0.1, 0.2, 0.5, 1, 2 and 3 C, respectively. This reduced polarization was beneficial from the conductive $Li_4Ti_5O_{12}$ layer coated on the surface of $LiNi_{0.5}Co_{0.2}Mn_{0.3}O_2$ particles, which promoted the kinetics of Li^+ extraction/insertion. (Thackeray and Amine, 2021). $Li_4Ti_5O_{12}$–coated $Li_{1.1}Ni_{0.35}Mn_{0.55}O_2$ cathode exhibits a superior long–term cycling performance for 100 cycles at the 1 C rate, the specific capacity of $Li_4Ti_5O_{12}$–coated $Li_{1.1}Ni_{0.35}Mn_{0.55}O_2$ cathode shows an increase in the first several cycles. This is beneficial from the protective layer that provides an activation of the cathode materials. The $Li_4Ti_5O_{12}$–coated $Li_{1.1}Ni_{0.35}Mn_{0.55}O_2$ cathode shows a specific discharge capacity of 113.5 mAh g^{-1} after 100 cycles. However, the specific discharge capacity of pristine $Li_{1.1}Ni_{0.35}Mn_{0.55}O_2$ cathode was 95.2 mAh g^{-1} after the identical operation process. It is considered that the coating layer of spinel $Li_4Ti_5O_{12}$ provides stable interfacial reaction kinetics for $Li_{1.1}Ni_{0.35}Mn_{0.55}O_2$ cathode, which decreases the loss of irreversible capacity.

It is known that the layered Li–rich cathode materials exhibit a large capacity fade at high voltages because of dissolution of the transition metals and the attack by liquid electrolytes. In order to study the effect of coating for the high–voltage stability of the cathode materials, the electrochemical performance of pristine $Li_{1.1}Ni_{0.35}Mn_{0.55}O_2$ and $Li_4Ti_5O_{12}$–coated $Li_{1.1}Ni_{0.35}Mn_{0.55}O_2$ cathode at 0.1 C with various upper cutoff voltages were also evaluated. As shown in **Figure 3**, higher discharge capacities were

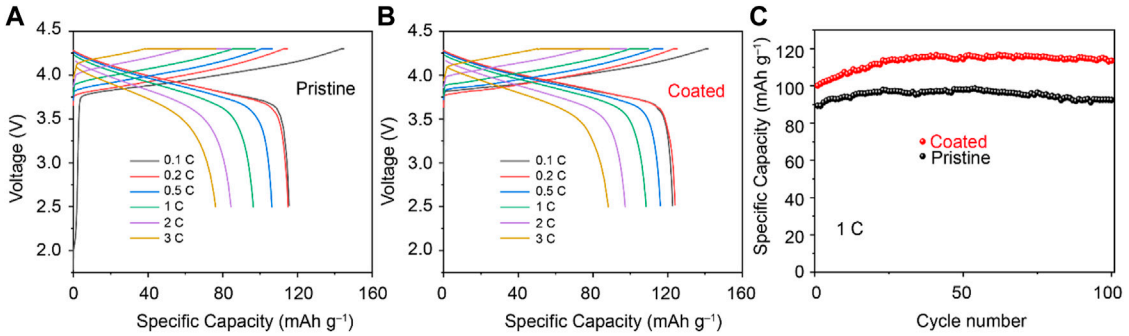

FIGURE 2 | Initial charge/discharge voltage profiles of **(A)** pristine $Li_{1.1}Ni_{0.35}Mn_{0.55}O_2$ cathodes and **(B)** $Li_4Ti_5O_{12}$–coated $Li_{1.1}Ni_{0.35}Mn_{0.55}O_2$ cathodes. **(C)** Long–term cycling performance of $Li_4Ti_5O_{12}$–coated $Li_{1.1}Ni_{0.35}Mn_{0.55}O_2$ and $Li_{1.1}Ni_{0.35}Mn_{0.55}O_2$ cathodes.

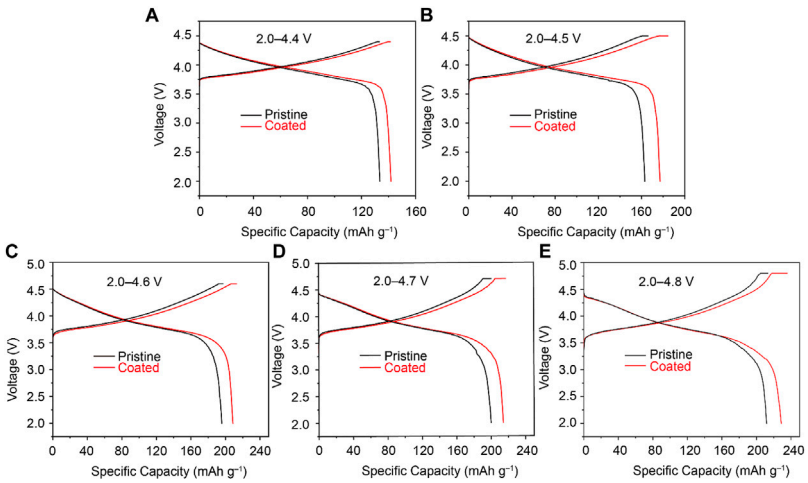

FIGURE 3 | Cycling performance of $Li_4Ti_5O_{12}$–coated $Li_{1.1}Ni_{0.35}Mn_{0.55}O_2$ (Coated) and $Li_{1.1}Ni_{0.35}Mn_{0.55}O_2$ cathodes (Pristine) with various upper cutoff voltages.

obtained for all samples with increased upper cutoff voltages. For instance, in the charge/discharge voltage range of 2.0–4.4 V (**Figure 3A**), the discharge capacities of the $Li_4Ti_5O_{12}$–coated $Li_{1.1}Ni_{0.35}Mn_{0.55}O_2$ and pristine $Li_{1.1}Ni_{0.35}Mn_{0.55}O_2$ are 141.9 and 133.6 mAh g^{-1}, respectively. The discharge capacities of 177.1, 208.6, 214.2, and 228.6 mAh g^{-1} are obtained with upper cutoff voltages of 4.5, 4.6, 4.7, and 4.8 V for $Li_4Ti_5O_{12}$–coated $Li_{1.1}Ni_{0.35}Mn_{0.55}O_2$ cathode, whereas the pristine $Li_{1.1}Ni_{0.35}Mn_{0.55}O_2$ cathodes only deliver 163.0, 195.7, 200.0, and 211.7 mAh g^{-1}, respectively. The initial irreversible capacities of $Li_4Ti_5O_{12}$–coated $Li_{1.1}Ni_{0.35}Mn_{0.55}O_2$ cathode were reduced in comparison with the pristine $Li_{1.1}Ni_{0.35}Mn_{0.55}O_2$ under increased upper cutoff potential. These results demonstrated that the $Li_4Ti_5O_{12}$ coating on the $Li_{1.1}Ni_{0.35}Mn_{0.55}O_2$ coating plays a barrier to protect the cathode materials from the transition metal dissolution at a high delithiation state; in addition, electrolyte corrosion and the volume expansion/contraction of the cathode were alleviated owing to the superb integrity of the $Li_4Ti_5O_{12}$ coating material.

In **Figure 4A**, the Nyquist plots of the cells at the 2nd and the 50th cycle are compared. The semicircle in high frequency represents the solid electrolyte interface resistance (R_{sf}), which includes the lithium ions transfer through the electrode material, the coating layer, and solid electrolyte interphase during cycling. The semicircle in low frequency is assigned to the charge transfer resistance at the interface of cathode/electrolyte (R_{ct}) (Reddy et al., 2007). $Li_4Ti_5O_{12}$–coated $Li_{1.1}Ni_{0.35}Mn_{0.55}O_2$ cathode shows initial smaller resistances than the counterpart; after the 50th cycle, all the resistances grow as a result of cycling degradation. The smaller increment of $Li_4Ti_5O_{12}$–coated $Li_{1.1}Ni_{0.35}Mn_{0.55}O_2$ cathode than pristine cathode reflects less side reaction at the electrode/electrolyte interface, reflecting the inhabitation of the excessive formation of solid electrolyte interfaces (SEI) and cathode electrolyte interfaces (CEI) between the electrolyte and the electrodes. These results demonstrated that the coating inhibits the decomposition of electrolyte by the reductive lithium metal and high oxidative cathode during cycling (Zha et al., 2022). The ionic conductive $Li_4Ti_5O_{12}$ alleviates the increase in impedance and substantial cycling deterioration.

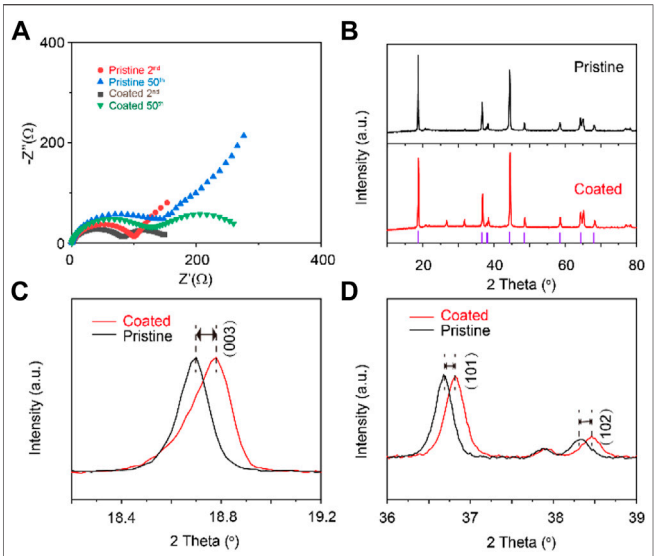

FIGURE 4 | Comparison of **(A)** EIS curves and **(B–D)** XRD patterns of $Li_4Ti_5O_{12}$–coated $Li_{1.1}Ni_{0.35}Mn_{0.55}O_2$ and $Li_{1.1}Ni_{0.35}Mn_{0.55}O_2$ cathodes after cycles.

The *ex–situ* XRD patterns of the $Li_{1.1}Ni_{0.35}Mn_{0.55}O_2$ electrodes after cycles were recorded. The main diffraction peaks can be indexed into the layered α–$NaFeO_2$ structure with a space group of R3̄m. No new phases were identified for the sample with lithium–and titanium–containing coating, which may be attributed to the small amount of lithium–and titanium–containing coating or amorphous state under the detection revolution of XRD (Zhang et al., 2013; Ahaliabadeh et al., 2021). As shown in **Figures 4C,D**, the (003) and (101) peaks of the pristine sample shifted slightly toward the lower angle, reflecting the destruction of the crystal structure of the pristine sample during the charge and discharge process. In contrast, the $Li_4Ti_5O_{12}$–coated $Li_{1.1}Ni_{0.35}Mn_{0.55}O_2$ cathode restrained good structure stability during cycling.

SEM images of the $Li_4Ti_5O_{12}$–coated $Li_{1.1}Ni_{0.35}Mn_{0.55}O_2$ and $Li_{1.1}Ni_{0.35}Mn_{0.55}O_2$ cathodes after cycling are performed and shown in **Figure 5**. The surface crack could be seen from the $Li_{1.1}Ni_{0.35}Mn_{0.55}O_2$ cathodes after cycling, while the $Li_4Ti_5O_{12}$–coated $Li_{1.1}Ni_{0.35}Mn_{0.55}O_2$ presents the original spherical morphology (**Figures 5A,B**). The elemental mapping displayed in **Figure 5E** confirms that Ti is uniformly dispersed on the particles. The results demonstrated that the $Li_4Ti_5O_{12}$ plays a significant role in protecting the $Li_{1.1}Ni_{0.35}Mn_{0.55}O_2$ particles from the structure cracks and the electrolyte corrosion.

In addition, the cycling stability of the $Li_{1.1}Ni_{0.35}Mn_{0.55}O_2$ electrodes with/without coating were investigated in the all–solid–state lithium batteries with polymer electrolytes. The Nyquist plots in **Figure 6A** exhibit a smaller total resistance of the all–solid–state using $Li_4Ti_5O_{12}$–coated $Li_{1.1}Ni_{0.35}Mn_{0.55}O_2$ electrode. **Figure 6B** shows the initial galvanostatic curves of $Li_4Ti_5O_{12}$–coated $Li_{1.1}Ni_{0.35}Mn_{0.55}O_2$ electrodes in all–solid–state batteries cycling at 0.05, 0.1, 0.2 mA cm^{-2} in the voltage range of 2.8–4.3 V at 60°C. The initial discharge capacities of $Li_4Ti_5O_{12}$–coated $Li_{1.1}Ni_{0.35}Mn_{0.55}O_2$ electrodes are 151, 138, and 123 mAh g^{-1}, respectively.

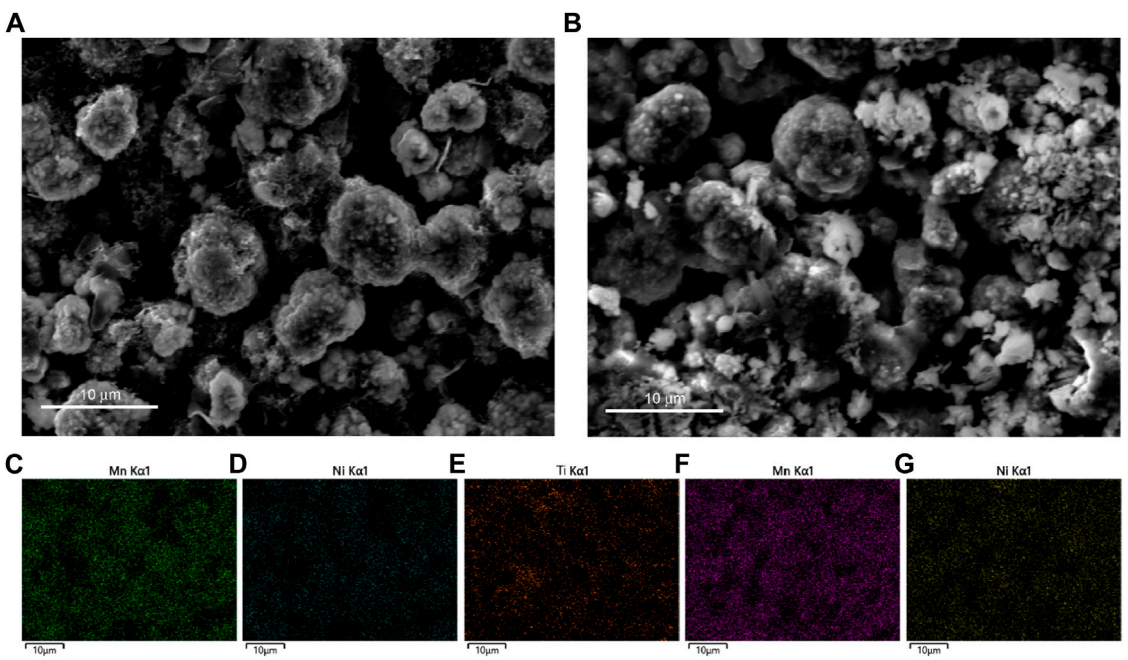

FIGURE 5 | SEM and EDS mapping images of $Li_4Ti_5O_{12}$–coated $Li_{1.1}Ni_{0.35}Mn_{0.55}O_2$ **(A,C,D,E)** and $Li_{1.1}Ni_{0.35}Mn_{0.55}O_2$ cathodes after cycles **(B,F,G)**.

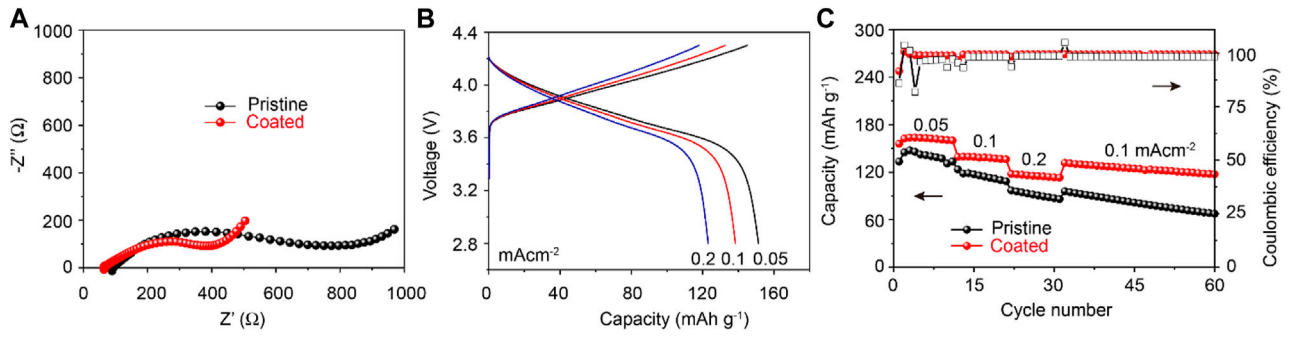

FIGURE 6 | (A) EIS plots of the all–solid–state cells using $Li_{1.1}Ni_{0.35}Mn_{0.55}O_2$ with/without $Li_4Ti_5O_{12}$ coating **(B)** Initial charge and discharge curves of $Li_4Ti_5O_{12}$–coated $Li_{1.1}Ni_{0.35}Mn_{0.55}O_2$/Li all–solid–state cells **(C)** Coulombic efficiency and rate performance of all–solid–state batteries using $Li_4Ti_5O_{12}$–coated $Li_{1.1}Ni_{0.35}Mn_{0.55}O_2$ electrodes.

The rate performances of pristine and $Li_4Ti_5O_{12}$–coated $Li_{1.1}Ni_{0.35}Mn_{0.55}O_2$ electrodes are compared in **Figure 6C**. It reveals that the $Li_4Ti_5O_{12}$–coated $Li_{1.1}Ni_{0.35}Mn_{0.55}O_2$ electrodes delivers higher discharge capacities compared with those of pristine electrode at 0.05, 0.1, 0.2 mA cm^{-2} for 10 cycles, indicating that $Li_4Ti_5O_{12}$ coating effectively improves the rate performance of Li–rich material. The pristine and $Li_4Ti_5O_{12}$–coated $Li_{1.1}Ni_{0.35}Mn_{0.55}O_2$ electrodes exhibit the Coulombic efficiency of 98.5 and 99.4%, respectively. Furthermore, the discharge capacity can be recovered entirely when the current density is back to 0.1 mA cm^{-2}, implying that the $Li_4Ti_5O_{12}$–coated $Li_{1.1}Ni_{0.35}Mn_{0.55}O_2$ electrode has desirable electrochemical reversibility and structural stability in all–solid–state lithium batteries. The capacity retention of $Li_4Ti_5O_{12}$–coated $Li_{1.1}Ni_{0.35}Mn_{0.55}O_2$ electrodes in the all–solid–state battery 89.3% at a current density of 0.1 mA cm^{-2} for 60 cycles. The improved discharge capacity and cycle stability of $Li_4Ti_5O_{12}$–coated $Li_{1.1}Ni_{0.35}Mn_{0.55}O_2$ electrodes in the solid–state batteries can be ascribed to the high Li^+ ionic conductive $Li_4Ti_5O_{12}$ coating.

CONCLUSION

The electrochemical properties of pristine and $Li_4Ti_5O_{12}$–coated $Li_{1.1}Ni_{0.35}Mn_{0.55}O_2$ electrodes at high upper cutoff voltages and solid–state batteries were compared at room temperature and 60°C. The experimental results demonstrate that the $Li_4Ti_5O_{12}$ coating layer is effective in stabilizing the $Li_{1.1}Ni_{0.35}Mn_{0.55}O_2$ crystal structure and providing fast lithium transfer at the electrode/electrolyte interface during charge/discharge cycles. The improved structural integrity and enhanced ionic conductivity of the $Li_4Ti_5O_{12}$–coated $Li_{1.1}Ni_{0.35}Mn_{0.55}O_2$ electrodes show improved cycling performance at high upper cutoff voltages. When assembled in an all–solid–state battery with polymer electrolyte, the $Li_4Ti_5O_{12}$–coated $Li_{1.1}Ni_{0.35}Mn_{0.55}O_2$ electrode still exhibits a better cyclability than the pristine $Li_{1.1}Ni_{0.35}Mn_{0.55}O_2$ electrode, demonstrating attractive application in electrode material design and optimization for LIBs.

DATA AVAILABILITY STATEMENT

The original contributions presented in the study are included in the article/Supplementary Material, further inquiries can be directed to the corresponding author.

AUTHOR CONTRIBUTIONS

WH conceived the project, and performed the data analysis and wrote the manuscript. SZ supervised the project. TY and XR conducted the material synthesis and conventional battery experiments. MZ conducted the all-solid-state lithium battery tests. All authors edited the manuscript.

FUNDING

The work was supported by the funding from the National Natural Science Foundation of China (Grant No. 51874151).

REFERENCES

Ahaliabadeh, Z., Miikkulainen, V., Mäntymäki, M., Mousavihashemi, S., Lahtinen, J., Lide, Y., et al. (2021). Understanding the Stabilizing Effects of Nanoscale Metal Oxide and Li-Metal Oxide Coatings on Lithium-Ion Battery Positive Electrode Materials. *ACS Appl. Mater. Inter.* 13, 42773–42790. doi:10.1021/acsami.1c11165

de Biasi, L., Schwarz, B., Brezesinski, T., Hartmann, P., Janek, J., and Ehrenberg, H. (2019). Chemical, Structural, and Electronic Aspects of Formation and Degradation Behavior on Different Length Scales of Ni-Rich NCM and Li-Rich HE-NCM Cathode Materials in Li-Ion Batteries. *Adv. Mater.* 31, e1900985. doi:10.1002/adma.201900985

Herzog, M. J., Esken, D., and Janek, J. (2021a). Improved Cycling Performance of High-Nickel NMC by Dry Powder Coating with Nanostructured Fumed

Al_2O_3, TiO_2, and ZrO_2: A Comparison. *Batteries & Supercaps* 4, 1003–1017. doi:10.1002/batt.202100016

Herzog, M. J., Gauquelin, N., Esken, D., Verbeeck, J., and Janek, J. (2021b). Facile Dry Coating Method of High-Nickel Cathode Material by Nanostructured Fumed Alumina (Al_2O_3) Improving the Performance of Lithium-Ion Batteries. *Energy Tech* 9, 2100028. doi:10.1002/ente.202100028

Herzog, M. J., Gauquelin, N., Esken, D., Verbeeck, J., and Janek, J. (2021c). Increased Performance Improvement of Lithium-Ion Batteries by Dry Powder Coating of High-Nickel NMC with Nanostructured Fumed Ternary Lithium Metal Oxides. *ACS Appl. Energ. Mater.* 4, 8832–8848. doi:10.1021/acsaem.1c00939

Hu, M., Pang, X., and Zhou, Z. (2013). Recent Progress in High-Voltage Lithium Ion Batteries. *J. Power Sourc.* 237, 229–242. doi:10.1016/j.jpowsour.2013.03.024

Jia, Y., He, G., Hu, W., Yang, H., Yang, Z., Yu, H., et al. (2018). The Effects of Oxygen in Spinel Oxide $Li_{1+x}Ti_{2-x}O_4$-$_\delta$ Thin Films. *Sci. Rep.* 8, 3995. doi:10.1038/s41598-018-22393-8

Jiang, Q., Wang, X., Zhang, Y., Yuan, N., and Tang, J. (2020). High Efficient and Environment Friendly Plasma-Enhanced Synthesis of Al_2O_3-Coated $LiNi_{1/3}Co_{1/3}Mn_{1/3}O_2$ with Excellent Electrochemical Performance. *Front. Chem.* 8, 72. doi:10.3389/fchem.2020.00072

Jung, S.-K., Gwon, H., Hong, J., Park, K.-Y., Seo, D.-H., Kim, H., et al. (2014). Understanding the Degradation Mechanisms of $LiNi_{0.5}Co_{0.2}Mn_{0.3}O_2$ Cathode Material in Lithium Ion Batteries. *Adv. Energ. Mater.* 4, 1300787. doi:10.1002/aenm.201300787

Kalluri, S., Yoon, M., Jo, M., Liu, H. K., Dou, S. X., Cho, J., et al. (2017). Feasibility of Cathode Surface Coating Technology for High-Energy Lithium-Ion and Beyond-Lithium-Ion Batteries. *Adv. Mater.* 29, 1605807. doi:10.1002/adma.201605807

Lin, X., Sun, Y., Liu, Y., Jiang, K., and Cao, A. (2021). Stabilization of High-Energy Cathode Materials of Metal-Ion Batteries: Control Strategies and Synthesis Protocols. *Energy Fuels* 35, 7511–7527. doi:10.1021/acs.energyfuels.1c00493

Liu, Y., Lin, X. J., Sun, Y. G., Xu, Y. S., Chang, B. B., Liu, C. T., et al. (2019). Precise Surface Engineering of Cathode Materials for Improved Stability of Lithium-Ion Batteries. *Small* 15, e1901019. doi:10.1002/smll.201901019

Liu, Z., Huang, Y., Huang, Y., Yang, Q., Li, X., Huang, Z., et al. (2020). Voltage Issue of Aqueous Rechargeable Metal-Ion Batteries. *Chem. Soc. Rev.* 49, 180–232. doi:10.1039/c9cs00131j

Nayak, P. K., Erickson, E. M., Schipper, F., Penki, T. R., Munichandraiah, N., Adelhelm, P., et al. (2018). Review on Challenges and Recent Advances in the Electrochemical Performance of High Capacity Li- and Mn-Rich Cathode Materials for Li-Ion Batteries. *Adv. Energ. Mater.* 8, 1702397. doi:10.1002/aenm.201702397

Nisar, U., Petla, R., Jassim Al-Hail, S. A., Quddus, A. A., Monawwar, H., Shakoor, A., et al. (2020). Impact of Surface Coating on Electrochemical and thermal Behaviors of a Li-Rich $Li_{1.2}Ni_{0.16}Mn_{0.56}Co_{0.08}O_2$ Cathode. *RSC Adv.* 10, 15274–15281. doi:10.1039/d0ra02060e

Reddy, M. V., Subba Rao, G. V., and Chowdari, B. V. R. (2007). Preparation and Characterization of $LiNi_{0.5}Co_{0.5}O_2$ and $LiNi_{0.5}Co_{0.4}Al_{0.1}O_2$ by Molten Salt Synthesis for Li Ion Batteries. *J. Phys. Chem. C* 111, 11712–11720. doi:10.1021/jp0676890

Sharifi-Asl, S., Lu, J., Amine, K., and Shahbazian-Yassar, R. (2019). Oxygen Release Degradation in Li-Ion Battery Cathode Materials: Mechanisms and Mitigating Approaches. *Adv. Energ. Mater.* 9, 1900551. doi:10.1002/aenm.201900551

Shi, J. L., Xiao, D. D., Ge, M., Yu, X., Chu, Y., Huang, X., et al. (2018). High-Capacity Cathode Material with High Voltage for Li-Ion Batteries. *Adv. Mater.* 30, 1705575. doi:10.1002/adma.201705575

Sun, H. H., Kim, U.-H., Park, J.-H., Park, S.-W., Seo, D.-H., Heller, A., et al. (2021a). Transition Metal-Doped Ni-Rich Layered Cathode Materials for Durable Li-Ion Batteries. *Nat. Commun.* 12, 6552. doi:10.1038/s41467-021-26815-6

Sun, J., Sheng, C., Cao, X., Wang, P., He, P., Yang, H., et al. (2021b). Restraining Oxygen Release and Suppressing Structure Distortion in Single-Crystal Li-Rich Layered Cathode Materials. *Adv. Funct. Mater.*, 2110295. doi:10.1002/adfm.202110295

Thackeray, M. M., and Amine, K. (2021). $Li_4Ti_5O_{12}$ Spinel Anodes. *Nat. Energ.* 6, 683. doi:10.1038/s41560-021-00829-2

Wang, C.-C., Lin, J.-W., Yu, Y.-H., Lai, K.-H., Chiu, K.-F., and Kei, C.-C. (2018). Electrochemical and Structural Investigation on Ultrathin ALD ZnO and TiO_2 Coated Lithium-Rich Layered Oxide Cathodes. *ACS Sustain. Chem. Eng.* 6, 16941–16950. doi:10.1021/acssuschemeng.8b04285

Wang, C.-W., Zhou, Y., You, J.-H., Chen, J.-D., Zhang, Z., Zhang, S.-J., et al. (2020a). High-Voltage LiCoO2 Material Encapsulated in a Li4Ti5O12Ultrathin Layer by High-Speed Solid-Phase Coating Process. *ACS Appl. Energ. Mater.* 3, 2593–2603. doi:10.1021/acsaem.9b02291

Wang, Y., Zhang, Q., Xue, Z. C., Yang, L., Wang, J., Meng, F., et al. (2020b). An *In Situ* Formed Surface Coating Layer Enabling $LiCoO_2$ with Stable 4.6 V High-Voltage Cycle Performances. *Adv. Energ. Mater.* 10, 2001413. doi:10.1002/aenm.202001413

Xia, Y., Zheng, J., Wang, C., and Gu, M. (2018). Designing Principle for Ni-Rich Cathode Materials with High Energy Density for Practical Applications. *Nano Energy* 49, 434–452. doi:10.1016/j.nanoen.2018.04.062

Xu, G. L., Liu, X., Daali, A., Amine, R., Chen, Z., and Amine, K. (2020). Challenges and Strategies to Advance High-Energy Nickel-Rich Layered Lithium Transition Metal Oxide Cathodes for Harsh Operation. *Adv. Funct. Mater.* 30, 2004748. doi:10.1002/adfm.202004748

Yan, H., Zhang, D., QiluDuo, X., Duo, X., and Sheng, X. (2021). A Review of Spinel Lithium Titanate ($Li_4Ti_5O_{12}$) as Electrode Material for Advanced Energy Storage Devices. *Ceramics Int.* 47, 5870–5895. doi:10.1016/j.ceramint.2020.10.241

Yi, T.-F., Yang, S.-Y., and Xie, Y. (2015). Recent Advances of $Li_4Ti_5O_{12}$ as a Promising Next Generation Anode Material for High Power Lithium-Ion Batteries. *J. Mater. Chem. A.* 3, 5750–5777. doi:10.1039/c4ta06882c

You, Y., and Manthiram, A. (2017). Progress in High-Voltage Cathode Materials for Rechargeable Sodium-Ion Batteries. *Adv. Energ. Mater.* 8, 1701785. doi:10.1002/aenm.201701785

Zha, Q., Hu, N., Song, C., Hou, H., Liao, S., and Zha, G. (2022). Improving Cycle Stability of Ni-Rich $LiNi_{0.8}Mn_{0.1}Co_{0.1}O_2$ Cathode Materials by $Li_4Ti_5O_{12}$ Coating. *Ionics* 28, 1047–1054. doi:10.1007/s11581-021-04375-5

Zhang, H., Deng, Q., Mou, C., Huang, Z., Wang, Y., Zhou, A., et al. (2013). Surface Structure and High-Rate Performance of Spinel $Li_4Ti_5O_{12}$ Coated with N-Doped Carbon as Anode Material for Lithium-Ion Batteries. *J. Power Sourc.* 239, 538–545. doi:10.1016/j.jpowsour.2013.03.013

Zhang, X., Sun, S., Wu, Q., Wan, N., Pan, D., and Bai, Y. (2015). Improved Electrochemical and thermal Performances of Layered Li $[Li_{0.2}Ni_{0.17}Co_{0.07}Mn_{0.56}]O_2$ via Li_2ZrO_3 Surface Modification. *J. Power Sourc.* 282, 378–384. doi:10.1016/j.jpowsour.2015.02.081

Zhou, A., Dai, X., Lu, Y., Wang, Q., Fu, M., and Li, J. (2016). Enhanced Interfacial Kinetics and High-Voltage/High-Rate Performance of $LiCoO_2$ Cathode by Controlled Sputter-Coating with a Nanoscale $Li_4Ti_5O_{12}$ Ionic Conductor. *ACS Appl. Mater. Inter.* 8, 34123–34131. doi:10.1021/acsami.6b11630

Conflict of Interest: The authors declare that the research was conducted in the absence of any commercial or financial relationships that could be construed as a potential conflict of interest.

Publisher's Note: All claims expressed in this article are solely those of the authors and do not necessarily represent those of their affiliated organizations, or those of the publisher, the editors and the reviewers. Any product that may be evaluated in this article, or claim that may be made by its manufacturer, is not guaranteed or endorsed by the publisher.